Check for updates

Received: 8 April 2018 | Accepted: 15 November 2018

DOI: 10.1002/jcb.28212

RESEARCH ARTICLE

WILEY Journal of Cellular Biochemistry

Changing expression profiles of mRNA, lncRNA, circRNA, and miRNA in lung tissue reveal the pathophysiological of bronchopulmonary dysplasia (BPD) in mouse model

Juan Wang[1,2] | Jing Yin[1] | Xingyun Wang[1] | Heng Liu[1] | Yin Hu[1] | Xiangyun Yan[1] | Bin Zhuang[1] | Zhangbin Yu[1] | Shuping Han[1]

[1]Department of Pediatrics, Women's Hospital of Nanjing Medical University, Nanjing Maternity and Child Health Care Hospital, Nanjing, Jiangsu, China

[2]Department of Pediatrics, The First People's Hospital of Lianyungang City, Lianyungang, Jiangsu, China

Correspondence
Zhangbin Yu, Ph.D., Department of Pediatrics, Women's Hospital of Nanjing Medical University, Nanjing Maternity and Child Health Care Hospital, 210004 Nanjing, Jiangsu, China.
Email: yuzhangbin@126.com
Shuping Han, Ph.D., MD., Department of Pediatrics, Women's Hospital of Nanjing Medical University, Maternity and Child Health Care Hospital, 210004 Nanjing, Jiangsu, China.
Email: shupinghan@njmu.edu.cn

Funding information
Nanjing Medical Science and Technique Development Foundation, Grant/Award Number: 201605052; National Natural Science Foundation of China, Grant/Award Number: No. 201605052

Abstract

New perinatal care technologies have improved the survival rate of preterm neonates, but the prevalence of bronchopulmonary dysplasia (BPD), one of the most intractable problems in neonatal intensive care unit (NICU), remains unchanged. In present study, high-throughput sequencing (HTS) was performed to detect the expression profiles of long noncoding RNAs (lncRNAs), messenger RNAs (mRNAs), circular RNAs (circRNAs), and microRNAs (miRNAs) in hyperoxia-induced BPD mouse model. Significant differentially expressed RNAs were selected and clustered between the BPD group and the control group. The results revealed that expressions of 1778 lncRNAs, 1240 mRNAs, 97 circRNAs, and 201 miRNAs were significantly altered in the BPD group. Gene ontology (GO) and Kyoto Encyclopedia of Genes and Genomes (KEGG) were performed to predict the potential functions of differentially expressed RNAs. lncRNA-mRNA and circRNA-miRNA coexpression networks were constructed to detect their association with the pathogenesis of BPD. Our study provides a systematic perspective on the potential function of RNAs during BPD.

KEYWORDS

bronchopulmonary dysplasia, circRNA, lncRNA, miRNA, mRNA

1 | INTRODUCTION

Bronchopulmonary dysplasia (BPD), is a common complication of preterm neonates, especially in those born with a lower gestational age (22-28 weeks) or birth weight (501–1500 g).[1] It brings negative effects on survival rate, life quality, and other long-term consequences of the patients.[2] The survival rate of the preterm neonates has been improved by new perinatal care technologies (such as use of pulmonary surfactant or antenatal steroids for lung maturation, invasive, and noninvasive ventilation, and other comprehensive therapies), but BPD has never shown a falling prevalence.[3,4] Now, it is still one of the most intractable problems in neonatal intensive care unit (NICU). Nowadays, the former "classic BPD" characterized by the injury of lung structure has advanced into "new BPD" that mainly damages the alveolar and vascular development.[3] However, the pathophysiology of BPD has not been well elucidated yet.

Genetic background is involved in the pathogenesis of BPD.[5] With high-throughput sequencing (HTS) and high-resolution microarray analysis, it is now possible to unveil

Juan Wang and Jing Yin authors have contributed equally to this study.

 © 2019 Wiley Periodicals, Inc.

the molecular mechanism of BPD. Noncoding RNAs (ncRNAs) considered as trash in a long time before are re-recognized as regulating molecules of many lung diseases in recent years. ncRNAs family mainly includes long noncoding RNA (lncRNA), microRNA (miRNA), and circularRNA (circRNA). Many studies have discovered the role of lncRNA, messenger RNA (mRNA), miRNA, or circRNA during pathogenesis of BPD.[6-9]

Competing endogenous RNAs (ceRNAs) are natural and intracellular miRNA inhibitors that compete to bind to miRNA recognition elements (MREs) to decrease miRNA availability and result in less mRNA repression.[10] Studies have revealed that ceRNA crosstalk is involved in many pathophysiological processes, which deepens our understanding on miRNA regulation.[11] The family of ceRNAs mainly includes lncRNA, miRNA, circRNA, and mRNA.

Thus, we designed our experiment. First, establishing a BPD animal model; then sequencing the expression profiles of lncRNA, mRNA, circRNA, and miRNA in lung tissues of hyperoxia-induced BPD mice and air-exposure mice; analyzing the function of these RNAs with Gene ontology (GO) and Kyoto Encyclopedia of Genes and Genomes (KEGG); finally, constructing lncRNA-mRNA and circRNA-miRNA coexpression networks to find some genes that might be associated with the pathogenesis of BPD. To the best of our knowledge, there is no report on the whole expression profiles of these RNAs in BPD model.

2 | MATERIALS AND METHODS

2.1 | Animal model

Pregnant C57BL/6J mice of similar gestation age were purchased from the Experimental Animal Center of Nanjing Medical University. Newborn mice in postnatal 24 hours were randomly assigned to room air (21% O_2) and hyperoxia (85% O_2) for 9 days. The room air group and hyperoxia group contained the same number of mice and were treated with the same nursing efforts. We prepared a man-made and well-sealed plexiglas chamber with sodium lime on the bottom for assuring the CO_2 concentration inside. The chamber was maintained at a temperature of 22°C to 26°C, a humidity of 50%-60%, and a CO_2 concentration of $< 0.5\%$. To create a hyperoxic environment, we aerated oxygen into the box and monitored its concentration with an oxygen meter. Nursing dams were exchanged every 24 hours so as to prevent oxygen toxicity.

On day 3, 6, and 9, three mice in each group were killed. Their lungs were collected and stored at −80°C or fixed in 4% paraformaldehyde for further usage. The whole study was approved by the Institutional Animal Care and Use Committee of Nanjing Medical University, and all the processes were done in accordance with the institutional guidelines for animal care.

2.2 | Hematoxylin & eosin (H&E) staining and immunohistochemistry

The fixed lung tissues were dehydrated in a series of ethanol, then embedded in paraffin and cut into 4-μm sections. Having been treated with xylene and ethanol, washed with distilled water, the sections were stained with haematoxylin and eosin (H&E). After dehydration and mounting, sections were examined under a x200 light microscope and typical pictures were taken. On the surface of the sampled tissue, a straight line was drawn from the center point of the bronchiole to the nearest point at the margin of septum or pleura. The number of alveoli passed through by the line was counted. Three slices in each group were read, and each slice was counted for five times. The average number of alveoli was taken as the mouse Radial Alveolar Counts (RAC) value.

Four-micrometer thick sections were dried, deparaffinized, and rehydrated. Antigens were retrieved. Endogenous peroxide activity and nonspecific binding sites were blocked. Then, primary antibodies CD34 (Ab81289, Abcam, London, UK) and the secondary antibodies were incubated. Finally, the sections were stained with chromogen diaminobenzidine(DAB), counterstained with hematoxylin, and mounted. Appropriate positive and negative controls were used. Cytoplasm reactivity was considered indicative of positive staining. Sections were then observed and photographed under a x400 light microscope. The number of blood vessels stained was counted. Three slices in each group were read, and each slice was counted for five times. The average number was taken as the mouse Microvessel Density (MVD).

2.3 | RNA isolation

Total RNA was extracted from frozen samples using a TRIzol reagent (Invitrogen, Carlsbad, CA) according to the manufacturer's introductions. RNA purity was guaranteed with a NanoDrop ND-1000 spectrophotometer (Agilent, SantaClara, CA) to measure the absorbance ratios of OD260/OD280. Ratios (1.8:2.0) were thought to be qualified. The integrity of RNA was assessed by standard denaturing agarose gel electrophoresis.

2.4 | Reverse transcription-quantitative polymerase chain reaction (RT-qPCR)

Transforming growth factor β (TGF-β), insulin-like growth factor 1 (IGF-1), and vascular endothelial growth factor α (VEGF-α) were validated in lung tissue samples of the

10974644, 2019, 6, Downloaded from https://onlinelibrary.wiley.com/doi/10.1002/jcb.28212 by Edinburgh University Library, Wiley Online Library on [05/08/2024]. See the Terms and Conditions (https://onlinelibrary.wiley.com/terms-and-conditions) on Wiley Online Library for rules of use; OA articles are governed by the applicable Creative Commons License

TABLE 1 The primers sequence for reverse transcription quantitative polymerase chain reaction (RT-qPCR)

TGF-β	**Forward** **Reverse**	**5′-CCCGAAGCGGACTACTATGC-3′** **5′-GCTTCCCGAATGTCTGACGTA-3′**
IGF-1	Forward Reverse	5′-TTCAGTTCGTGTGTGGACCG-3′ 5′-GGGCACAGTACATCTCCAGTCTC-3′
VEGF-α	Forward Reverse	5′-GCCAGCACATAGGAGAGATGAG-3′ 5′-GGCTTTGTTCTGTCTTTCTTTGG-3′
GAPDH	Forward Reverse	5′-TGACCTCAACTACATGGTCTAC-3′ 5′-CTTCCCATTCTCGGCCTTG-3′

Abbreviations: GAPDH, glyceraldehyde-3-phosphate dehydrogenase; IGF-1, insulin-like growth factor 1; TGF-β, transforming growth factor β; VEGF-α, vascular endothelial growth factor α.

BPD and control groups by reverse transcription-quantitative polymerase chain reaction (RT-qPCR). RNAs were reverse-transcribed into complementary DNAs (cDNAs) using the PrimeScript™ II Reverse Transcriptase (Takara), according to the manufacturer's instructions. All primers used in the study are shown in Table 1. Q-PCR was performed with SYBR® Premix Ex Taq™ II (Takara, Dalian, China) on StepOnePlus™ Real-Time PCR System (ABI, Applied Biosystems, Foster City, CA). The PCR conditions were as follows: An initial denaturation step at 95°C for 5 minutes, followed by 40 cycles of 95°C for 10 seconds, and 60°C for 30 seconds. The results were analyzed using $2^{-\triangle\triangle CT}$. $\triangle CT = {}_{CT}$(target gene)$-{}_{CT}$(internal reference), $\triangle\triangle CT = {}_{\triangle CT}$(sample)$-{}_{\triangle CT}$(control). All experiments were performed in triplicate.

2.5 | Library preparation and sequencing of RNA

Three pairs of tissue samples of the two groups were used for hi-seq analysis in Nanjing Decode Genomics. First, total RNA was extracted and its ribosomal RNA (rRNA) was removed. The remaining RNAs were further processed according to the Illumina protocol. After cDNAs synthesis, they were sequenced with Illumina HiSeq 2000 (Illumina) using paired end (PE) sequencing strategy. The raw data was recorded. Then sequence quality was evaluated with the quality control software Fast QC and clean reads were available.

2.6 | RNA-seq analysis and quality assessment

Based on the filtered clean reads, Tophat software was used to compare the clean reads with the reference genome. The comparison parameter was –segment-length 25 –segment-mismatches 2, other parameters were default. RNA-seq overall quality was also evaluated to ensure the qualified sample.

2.7 | lncRNA, mRNA, circRNA, and miRNA prediction

2.7.1 | lncRNA

To detect novel lncRNAs from the finally assemblies, we compared the merged transcriptome to rat known gene annotation using cuffcompare.[12] As a result, the candidate novel transcripts can be detected by their locations compared with the reference genes.

2.7.2 | mRNA

During model species analysis, the mRNAs had been comprehensively included, so the mRNAs of the samples were not be predicted again, and only the expression level of each mRNA was directly identified.

2.7.3 | circRNA

We applied two algorithms to detect circRNAs, CIRI,[13] and KNIFE,[14] which is the combination with the most sensitivity and specificity. To ensure the high accuracy for the identification of circRNAs, we adopt three criteria to retain the high confidence circRNAs: (1) Kept the circRNAs identified by two algorithms; and (2) selected those circRNAs identified in ≥2 junction reads in both algorithms and decoy/circ read count ratio ≤0.1 and *P*-value ≥0.9 in KNIFE; and (3) both detected in all samples.

2.7.4 | miRNA

Map the small RNA tags to genome by SOAP to analyze their expression and distribution on the genome. Align small RNA to the miRNA precursor of corresponding species (mature miRNA if there is no precursor information of that species in miRBase21.0) to obtain the miRNA count. We developed a prediction software Mireap to predict novel miRNA by exploring the secondary structure, the Dicer cleavage site and the minimum free energy of the unannotated small RNA tags which could be mapped to genome.

2.8 | Screening and clustering analysis for differentially expressed lncRNA, mRNA, circRNA, and miRNA

The edgeR software was adopted for normalizing the raw data from each array. Expression difference of lncRNA, mRNA, circRNA, and miRNA was calculated. $P < 0.05$ was considered statistically different. Difference integration analysis (Venn analysis) was carried out with heat map, scatter plot, and venn diagram. Up or downregulated RNAs

10974644, 2019, 6, Downloaded from https://onlinelibrary.wiley.com/doi/10.1002/jcb.28212 by Edinburgh University Library, Wiley Online Library on [05/08/2024]. See the Terms and Conditions (https://onlinelibrary.wiley.com/terms-and-conditions) on Wiley Online Library for rules of use; OA articles are governed by the applicable Creative Commons License

were shown by pies with different colors. Differentially expressed lncRNAs, mRNAs, circRNAs, and miRNAs were analyzed using Cluster software.

2.9 | GO and KEGG pathway analysis

GO and KEGG pathway analyses were applied to predict the genes function. GO results were mainly classified into three subgroups namely biological process (BP), cellular component (CC), and molecular function (MF). Among them, we chose BP subgroup which is most involved in BPD to perform further analysis. The top 30 GO-BP terms and KEGG pathways were selected and ranked by enrich factor (EF). Then according to some literature review results, the top 10 regulated ones those may linked with BPD were available.

2.10 | lncRNA-mRNA coexpression network

According to the results from KEGG analysis, we drew out BPD-related pathways, through which the mRNAs and their corresponding lncRNAs were pinpointed. Finally, lncRNAs associated with these mRNAs were predicted.

2.11 | circRNA-miRNA coexpression network

Some circRNAs were obtained by screening host genes that may be related with BPD. From those having miRNA sponges, we screened out the circRNAs that can bind more than 10 miRNAs simultaneously. Pearson's correlation coefficient value of circRNA-miRNA coexpression network pairs was calculated, and strongly correlated pairs (>0.8 or <-0.8) were defined (either positive or negative).[15,16] Finally, 10 circRNAs and 52 coexpressed miRNAs were acquired.

3 | RESULTS

3.1 | Validation of hyperoxia-induced BPD animal model

No mice died in both groups. At day 3, 6, and 9 after birth, we compared the health status between the two groups. At 6 days after birth, mice in hyperoxia group showed less actions, low mood, and messy hair. At 9 days after birth, they showed obvious weight loss, disheveled hair, and strong anxiousness after the discontinuation of hyperoxia exposure. In the air group, mice showed normal growth, activity, hair, and response to stimulation. H&E staining results showed significant differences between the air group and the hyperoxia group (Figure 1), especially in the lung tissues of day 9. The structure, number, and septa of alveoli were normal in the air group. In the hyperoxia group, typical features of BPD were: Massive infiltration of red blood cells and inflammatory cells in alveolar cavities, widened alveolar septa, irregular alveolar structure and partial fusion, reduced alveolar number, and inflammatory atelectasis of some alveoli. All these features indicated that hyperoxia-induced BPD animal model had been successfully established.

There was no significant difference in RAC between the hyperoxia group and air group at 3 days after birth ($P>0.05$), but the difference was statistically significant ($P<0.05$) at 6 and 9 days after birth (Table 2, Figure 1). On day 3 after birth ($P>0.05$), there was no significant difference in MVD between the two groups, but on days 6 and 9 after birth ($P<0.05$), the difference was statistically significant ($P<0.05$) (Table 3, Figure 1). We also detected the differential expression levels of some well-known BPD biomarkers, such as TGF-β , IGF-1, and VEGF-α (Figure 1). TGF-β and IGF-1 increased obviously in the BPD group. In contrast, the mRNA level of VEGF-α decreased in BPD group.

3.2 | Expression profiles of lncRNAs and mRNAs in BPD model

Currently, it is well-known that lncRNA transcription usually regulates the expression of nearby protein-coding genes and targets distant activators or repressors to exert their biological function. Therefore, we compared differentially expressed lncRNAs with differentially expressed mRNAs for target prediction.[8] We identified a total of 26 784 lncRNAs and 12 964 mRNAs in all samples. The overlap of Venn diagram represents the undyregulated lncRNAs. Red and blue color represents up and downregulated lncRNAs, respectively. Two groups showed a total of differentially expressed 1778 lncRNAs (including significantly 874 upregulated and 904 downregulated) (Figure 2A-C), and 1240 mRNAs (including significantly 617 upregulated and 623 downregulated) (Figure 2D-F).

3.3 | Expression profiles of circRNAs and miRNAs in BPD model

Possible functions of circRNAs have been reported as regulators of splicing and transcription, miRNA sponges, protein binding, and RNA transport.[17-20] Among them, the function of miRNA sponges drew the most attention. That is why we analyze differentially expressed circRNAs with differentially expressed miRNAs. We identified a total of 1545 circRNAs and 634 miRNAs in all samples. The overlap of Venn diagram represents the undyregulated circRNAs and miRNAs. Red and blue color represents up

10974644, 2019, 6, Downloaded from https://onlinelibrary.wiley.com/doi/10.1002/jcb.28212 by Edinburgh University Library, Wiley Online Library on [05/08/2024]. See the Terms and Conditions (https://onlinelibrary.wiley.com/terms-and-conditions) on Wiley Online Library for rules of use; OA articles are governed by the applicable Creative Commons License

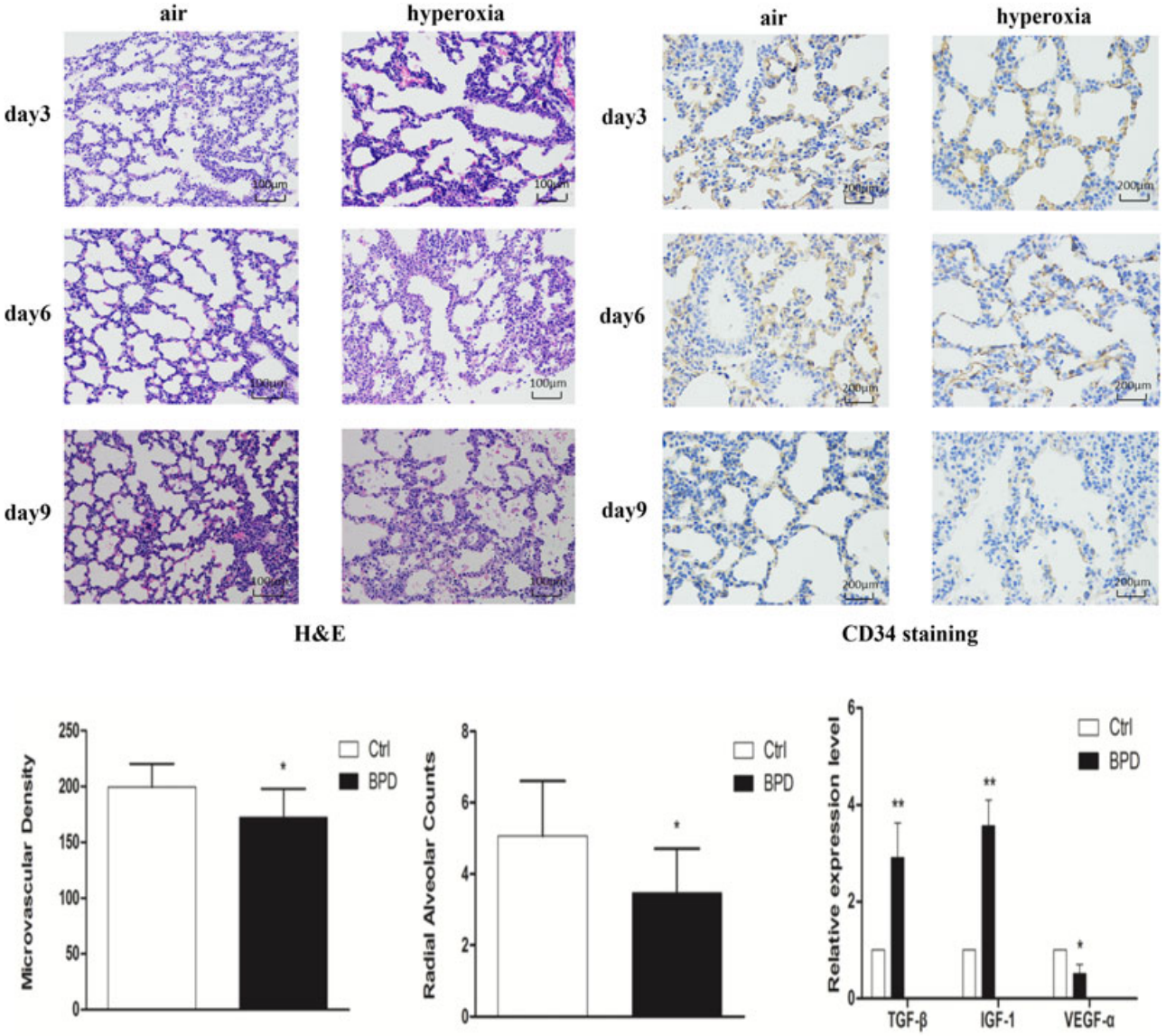

FIGURE 1 Validation of hyperoxia-induced BPD animal model H&E staining pathological pictures of lung samples at different time points in both groups (magnification, ×200). Calibration bar is 100 μm. Immunohistochemistry for CD34 in the lung samples at different time points in both groups (magnification, ×400). Calibration bar is 200 μm. The bars of RAC, MVD value on day 9 between BPD group and control group. Differential mRNA expression levels of TGF-β, IGF-1, VEGF-α between BPD group, and control group. BPD, bronchopulmonary dysplasia; Ctrl, control; IGF-1, insulin-like growth factor 1; MVD, microvascular density; RAC, radial alveolar counts; TGF-β, transforming growth factor β; VEGF-α, vascular endothelial growth factor α

and downregulated circRNAs and miRNAs, respectively. Two groups showed a total of differentially expressed 97 circRNAs (including significantly70 upregulated and 27 downregulated) (Figure 3A-C), and 201 miRNAs (including significantly 79 upregulated and 122 downregulated) (Figure 3D-F).

TABLE 2 Comparation of radial alveolar counts (RAC) value at different time points in both groups ($\bar{x} \pm s$)

Group	n	Day 3	Day 6	Day 9
Ctrl	3	(3.33 ± 1.59)	(4.47 ± 1.13)	(5.07 ± 1.53)
BPD	3	(3.40 ± 1.29)	(3.33 ± 1.49)	(3.47 ± 1.24)
t		−0.126	2.345	3.316
P		0.901	0.026	0.004

Abbreviations: BPD, bronchopulmonary dysplasia; Ctrl, control.

3.4 | GO and KEGG analysis of lnnRNA, circRNA, and miRNA

The top 10 enriched terms that may be associated with the mechanism of BPD were shown in Figure 4. According to the results, The most enriched and meaningful GO-BP terms and KEGG pathway analyses

10974644, 2019, 6, Downloaded from https://onlinelibrary.wiley.com/doi/10.1002/jcb.28212 by Edinburgh University Library, Wiley Online Library on [05/08/2024]. See the Terms and Conditions (https://onlinelibrary.wiley.com/terms-and-conditions) on Wiley Online Library for rules of use; OA articles are governed by the applicable Creative Commons License

TABLE 3 Comparation of microvascular density (MVD) value at different time points in both groups ($\bar{x} \pm s$)

Group	n	Day 3	Day 6	Day 9
Ctrl	3	(140.0 ± 40.95)	(172.07 ± 25.95)	(199.33 ± 21.07)
BPD	3	(131.53 ± 38.85)	(145.4 ± 37.67)	(172.27 ± 25.7)
t		0.581	2.258	3.154
P		0.566	0.032	0.004

Abbreviations: BPD, bronchopulmonary dysplasia; Ctrl, control.

were related to endothelial or epithelial cell development such as "regulation of endothelial cell development," "blood vessel endothelial cell proliferation," "vascular smooth muscle contraction," "EGFR tyrosine kinase inhibitor resistance," "bacterial invasion of epithelial cells," and "VEGF signaling pathway." On the other hand, "notch signaling pathway" was shown in both lncRNA and circRNA KEGG analysis results.

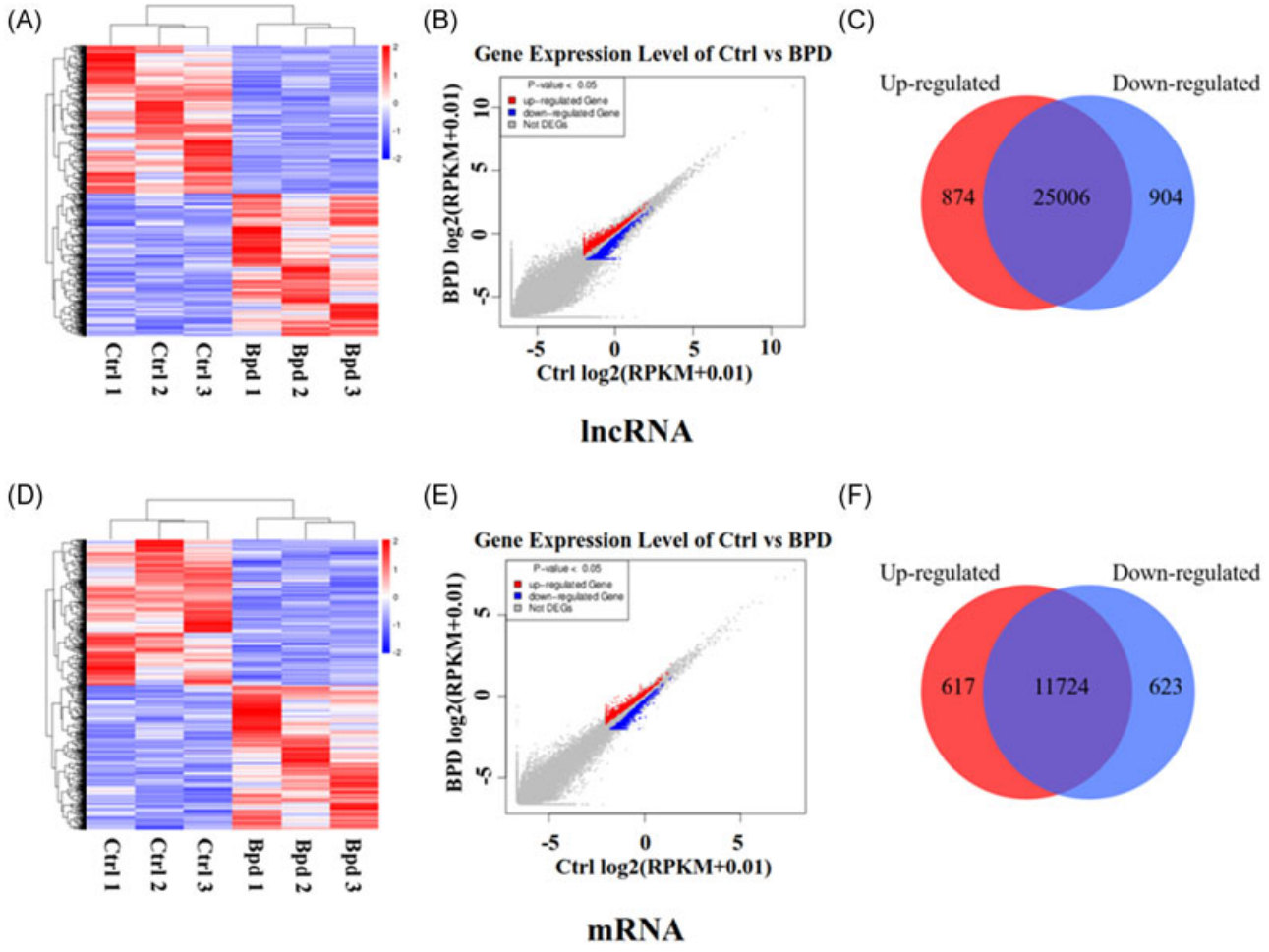

FIGURE 2 Differentially expressed lncRNAs and mRNAs between bronchopulmonary dysplasia (BPD) group and control (ctrl) group ($P < 0.05$). A, The cluster heat map of differentially expressed lncRNAs, red color represents upregulated lncRNAs, blue color represents downregulated lncRNAs, and heavier color represents higher fold change. B, Scatter plots showing differentially expressed lncRNAs between (BPD) group and control (ctrl) group. Red color represents upregulated lncRNAs and blue color represents downregulated lncRNAs. C, Venn analysis showing upregulated and downregulated lncRNAs in BPD group. D, The cluster heat map of differentially expressed mRNAs, red color represents upregulated mRNAs, blue color represents downregulated mRNAs, and heavier color represents higher fold change. E, Scatter plots showing differentially expressed mRNAs between (BPD) group and control (ctrl) group. Red color represents upregulated mRNAs and blue color represents downregulated mRNAs. F, Venn analysis showing upregulated and downregulated mRNAs in BPD group. lncRNAs, long noncoding RNAs; mRNAs, messenger RNAs

10974644, 2019, 6, Downloaded from https://onlinelibrary.wiley.com/doi/10.1002/jcb.28212 by Edinburgh University Library, Wiley Online Library on [05/08/2024]. See the Terms and Conditions (https://onlinelibrary.wiley.com/terms-and-conditions) on Wiley Online Library for rules of use; OA articles are governed by the applicable Creative Commons License

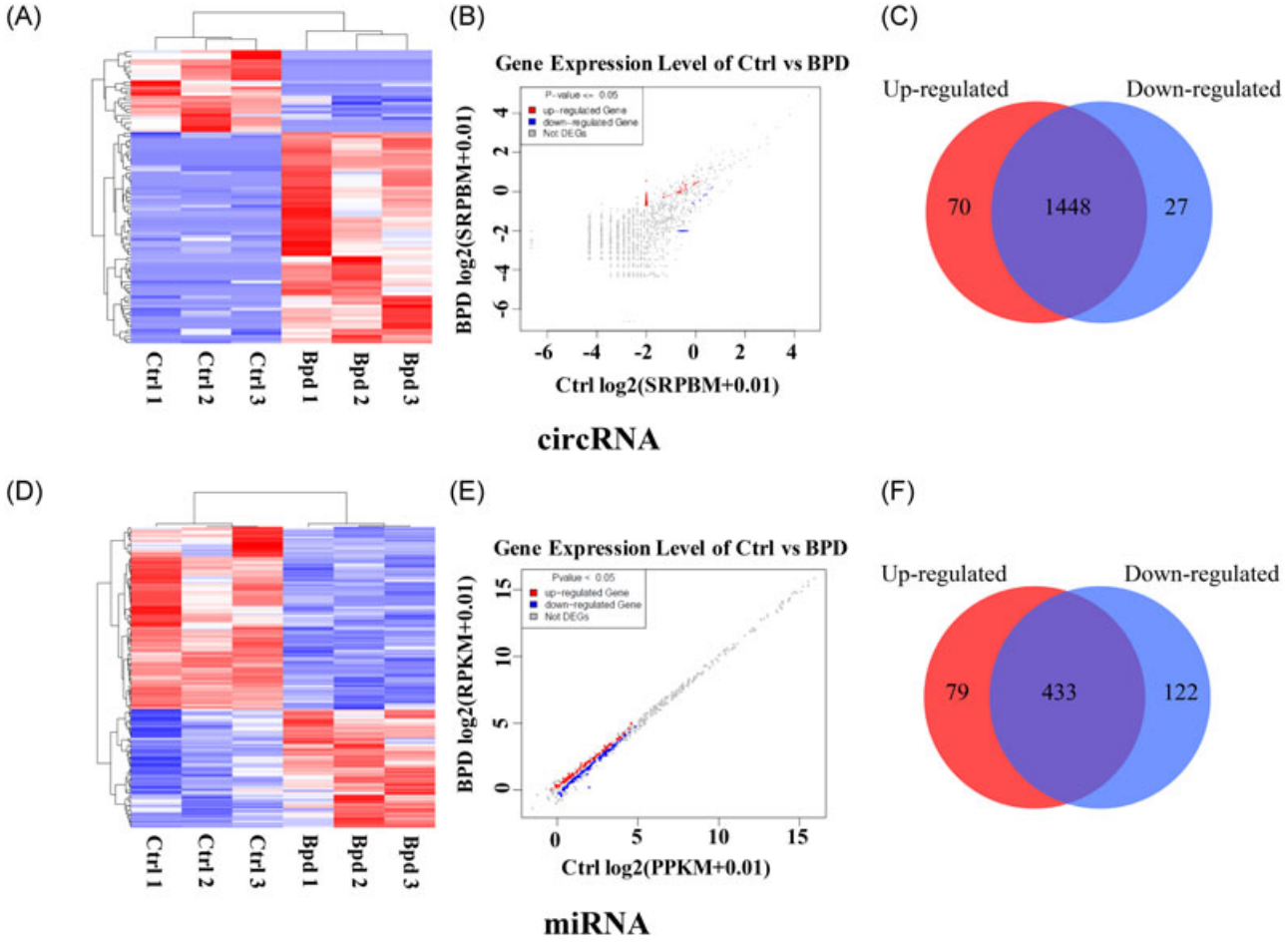

FIGURE 3 Differentially expressed circRNAs and miRNAs between bronchopulmonary dysplasia (BPD) group and control (ctrl) group ($P < 0.05$). A, The cluster heat map of differentially expressed circRNAs, red color represents upregulated circRNAs, green color represents downregulated lncRNAs, and heavier color represents higher fold change. B, Scatter plots showing differentially expressed circRNAs between (BPD) group and control (ctrl) group. Red color represents upregulated circRNAs and blue color represents downregulated circRNAs. C, Venn analysis showing upregulated and downregulated circRNAs in BPD group. D, The cluster heat map of differentially expressed miRNAs, red color represents upregulated miRNAs, green color represents downregulated miRNAs, and heavier color represents higher fold change. E, Scatter plots showing differentially expressed miRNAs between (BPD) group and control (ctrl) group. Red color represents upregulated miRNAs and blue color represents downregulated miRNAs. F, Venn analysis showing upregulated and downregulated miRNAs in BPD group. circRNAs, circular RNAs; miRNAs, microRNAs; lncRNAs, long noncoding RNAs

3.5 | Construction of the lncRNA-mRNA coexpression network

The lncRNA-mRNA coexpression network was constructed (Figure 5), and showed a complex interaction between lncRNAs and mRNAs. One lncRNA could regulate many genes in different ways and one gene could be regulated by many lncRNAs. Circle nodes represent lncRNA and square nodes represent mRNAs. Red color and green color of circle nodes represent the up or downregulation, respectively. The shade darkness of red and green represents fold change of lncRNAs. The size of circle represents *P*-value with larger size owing smaller *P*-value. Solid lines represent positive relationship and dash lines represent negative relationship. A total of 19 differentially expressed lncRNAs closely correlated with 31 mRNAs were defined. Among them, lncXLOC-020956, lncXLOC-067599, lncXLOC-131503, lncXLOC-061228, lncXLOC-133936, lncXLOC-010107, lncXLOC-036051, lncXLOC-012199, lncXLOC-078016, and lncXLOC-137636 were newly defined genes.

Furthermore, lncRNA XLOC-067599 interacted with six mRNAs, including epidermal growth factor-like 6 (EGFL6), IL2, IL20rb, IL22ra2, IL24, and vascular endothelial growth factor C (VEGFC), EGFL6, VEGFC may influence endothelial or epithelial cell development which is closely involved in alveoli and pulmonary vessels development during the BPD process.

10974644, 2019, 6, Downloaded from https://onlinelibrary.wiley.com/doi/10.1002/jcb.28212 by Edinburgh University Library, Wiley Online Library on [05/08/2024]. See the Terms and Conditions (https://onlinelibrary.wiley.com/terms-and-conditions) on Wiley Online Library for rules of use; OA articles are governed by the applicable Creative Commons License

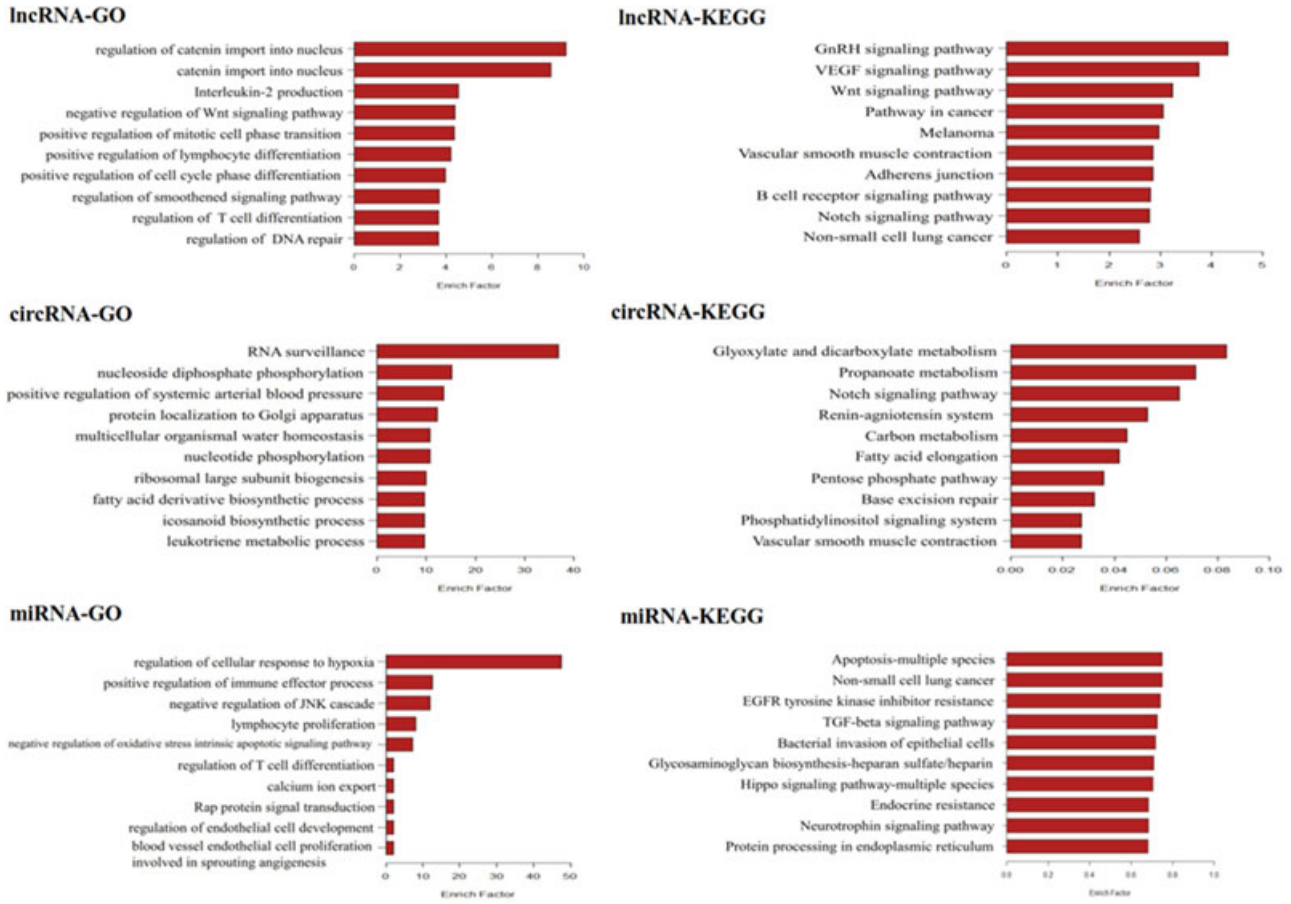

FIGURE 4 GO and KEGG analysis of lnnRNA, circRNA, and miRNA. The top 10 functional descriptors associated with BPD ranked by enrich factor, the abscissa represents the enrich factor and the ordinate represents the functional description. BPD, bronchopulmonary dysplasia; GO, Gene Ontology; KEGG, Kyoto Encyclopedia of Genes and Genomes

3.6 | Construction of the circRNA-miRNA coexpression network

Another circRNA-miRNA coexpression network was constructed (Figure 6). The network also showed a complex interaction between circRNAs and miRNAs. There exists a dominant circRNA-miRNA regulation network during the process of BPD. One circRNA could sponge many miRNAs and one miRNA could also regulate many circRNAs. In the network, circle represents miRNA and diamond represents circRNA. Up or downregulation are shown in yellow and blue color, respectively. Larger size of diamond represents higher fold change of circRNAs.

Furthermore, we can find that circRNAchr1:177096967|177109738 had a positive correlation with 21 miRNAs and negative correlation with 12 miRNAs. Among them, Xing et al[32] found that miR-33-5P, miR-25-3P, miR-92a-3P, miR-181b-5P, miR-34a-5P, and miR-22-3P were significantly differentially expressed in rat BPD model.

4 | DISCUSSION

BPD brings about high morbidity and mortality in NICU, and long-term consequences that may progress into the adulthood. However, the molecular pathways and cellular mechanisms that define BPD pathophysiology and progression are limited. Genetic variability is a main factor in the pathogenesis of BPD. Bhandari and Gruen first reviewed the genetics of BPD in 2006,[21] subsequently Shaw and O'Brodovich reviewed it in 2013.[22] From the review, a clearer understanding of genetic susceptibility for BPD has recently emerged. Incremental improvements will likely depend on identification of these genes for targeting specific therapies. HTS is a golden way for studying molecular mechanisms of diseases.[23] With it, the research on BPD can be improved.

To uncover the molecular mechanism of BPD, an animal model was constructed in this experiment. In the past decades, many kinds of animals have been used in

10974644, 2019, 6, Downloaded from https://onlinelibrary.wiley.com/doi/10.1002/jcb.28212 by Edinburgh University Library, Wiley Online Library on [05/08/2024]. See the Terms and Conditions (https://onlinelibrary.wiley.com/terms-and-conditions) on Wiley Online Library for rules of use; OA articles are governed by the applicable Creative Commons License

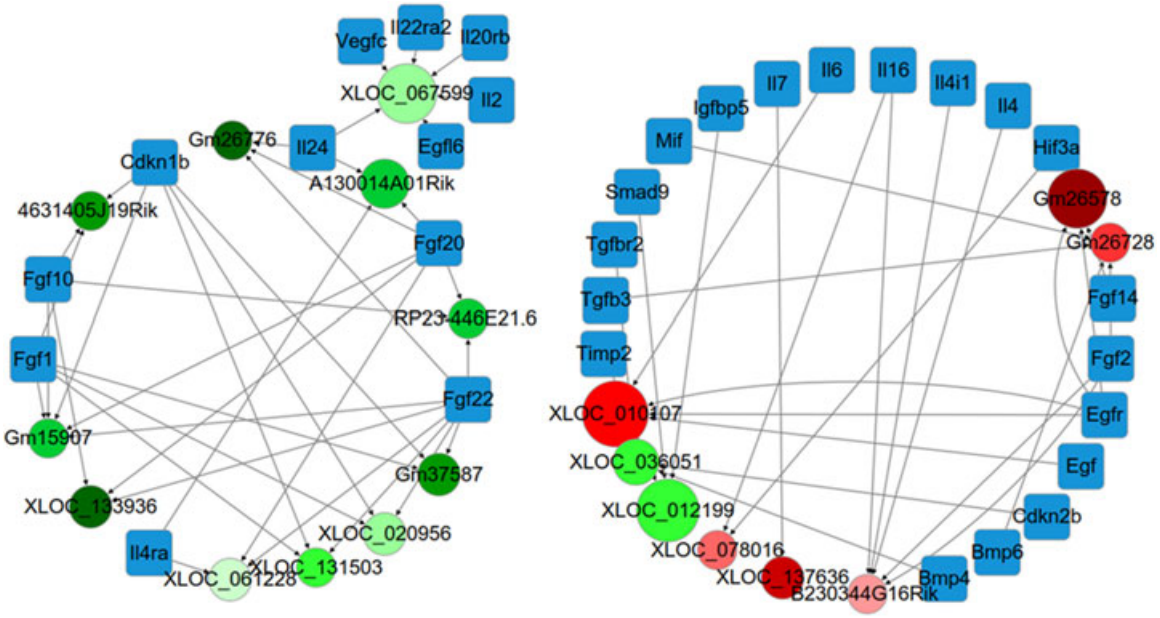

FIGURE 5 Construction of the lncRNA-mRNA coexpression network. A,B, Circle nodes represent lncRNA and square nodes represent mRNAs. Red color and green color of circle nodes represent up and downregulation, respectively. The shade darkness of red and green represents fold change of lncRNAs. The size of circle represents *P*-value with larger size owing smaller *P*-value. Solid lines represent positive relationship and dash lines represent negative relationship. lncRNAs, long noncoding RNAs; mRNA, messenger RNA

BPD models, like baboons, lambs, rabbits, pigs, mice, rats, and rodents.[6] Baboons and lambs are more physiologically close to human beings, but using them for medical purpose faces much criticism. Mice are easy to get and have a short gestational age. By consulting the literature, we learned that the lung development of the newborn mice is divided into three steps: Saccular phase (P0-P4), early alveolarization (P7), and bulk alveolarization (P14). The lung maturity of newborn mice within 24 hours is at the saccular stage which is accordant with the pathogenesis of new BPD.[24]

BPD model can be established through many ways. In models challenged with bleomycin[25] or endotoxin, the mortality is high and the mechanical ventilation is difficult.[26] But the hyperoxia model does not demonstrate this phenomenon. In this study, within 24 hours after the birth, C57BL/6J mice were exposed to hyperoxia to create an environment of BPD. The findings from H&E staining and immunohistochemistry after hyperoxia exposure indicated that the BPD animal model was successfully established. Further validation was performed by q-PCR, as we know, TGF-β can inhibit lung development and drive pulmonary fibrosis,[27] and IGF-1 can stimulated collagen synthesis.[28] These two factors increased obviously in the BPD group. In contrast, the mRNA level of VEGF-α which can regulate angiogenesis[29] decreased in the BPD group. All these changes can also be found in human BPD.

In our study, the expression profiles of lncRNA, mRNA, miRNA, and circRNA were detected in lung samples of the BPD group and the control group. From the results, we saw that thousands of lncRNAs, mRNAs, circRNAs, and miRNAs were differentially expressed compare with the control group. It is very interesting to notice that the expression patterns of lncRNAs and mRNAs were consistent, more downregulated transcripts and less upregulations (Figure 2). This result collaboratively explained that most of the current studies focused on the relationship between lncRNA-mRNA pairs. However, the expression patterns of circRNAs and miRNAs were not consistent (Figure 3), we analyzed that may be due to the insufficient number of detected circRNAs and miRNAs.

ncRNAs have been considered useless in cellular function in a long time, but nowadays mounting evidence shows that ncRNAs play an essential role.[30] There are many kinds of ncRNAs, including ribosomal rRNA, transfer RNA (tRNA), lncRNA, miRNA, and circRNA.[31] Pioneering studies were performed on the expression profile of lncRNAs in the BPD model.[8] Moreover, reports were made on the relationship between miRNAs and BPD,[32] relationships between circRNAs and lung adenocarcinoma, chronic thromboembolic pulmonary hypertension, and idiopathic lung fibrosis.[33-35] This is the first report on the changing expression of lncRNA, mRNA, circRNA, and miRNA in BPD. We aim to arouse the attention of ncRNAs regulation in studying the real molecular mechanism of BPD. Like the mechanism of ceRNA, they might work collaboratively.

10974644, 2019, 6, Downloaded from https://onlinelibrary.wiley.com/doi/10.1002/jcb.28212 by Edinburgh University Library, Wiley Online Library on [05/08/2024]. See the Terms and Conditions (https://onlinelibrary.wiley.com/terms-and-conditions) on Wiley Online Library for rules of use; OA articles are governed by the applicable Creative Commons License

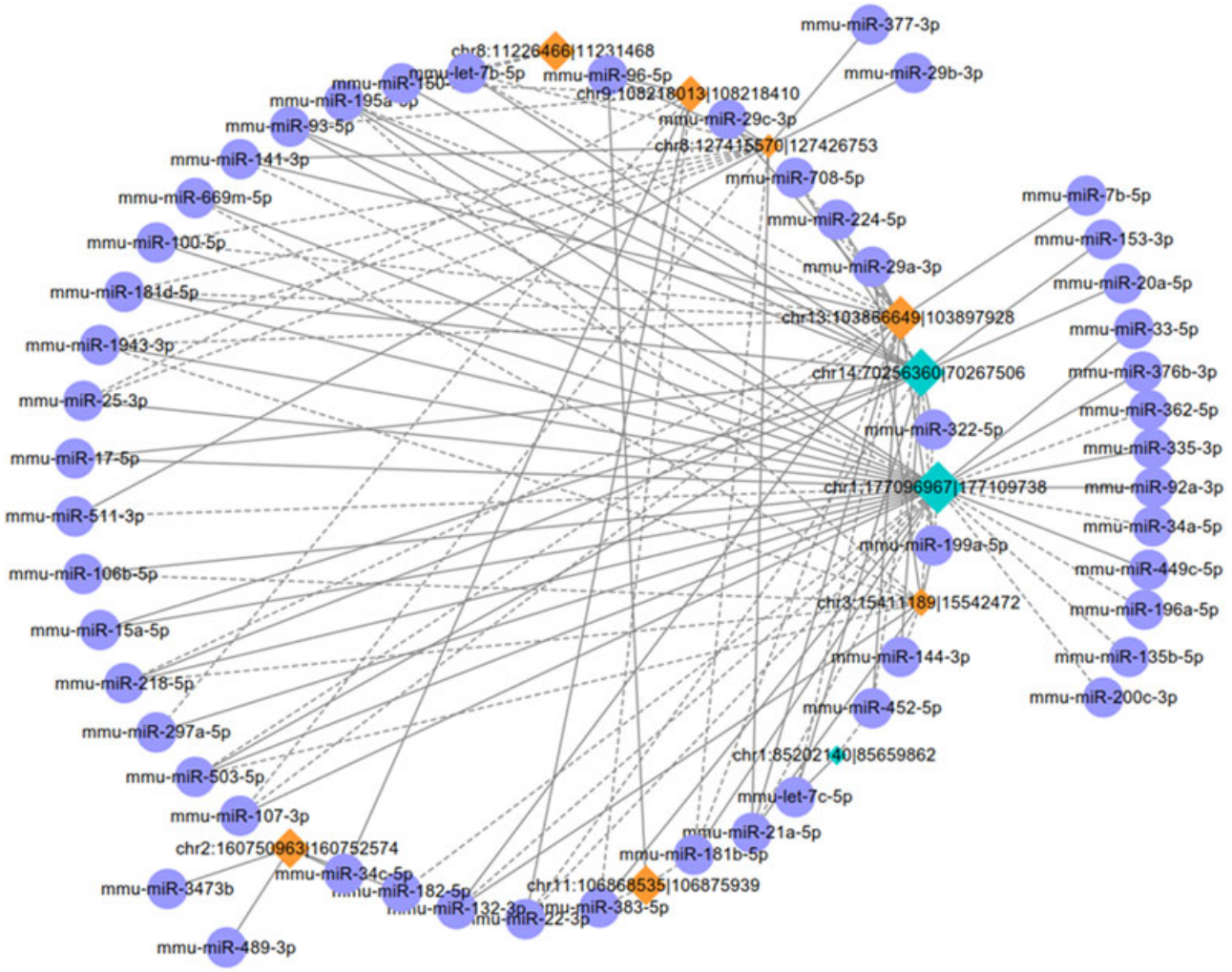

FIGURE 6 Construction of the circRNA-miRNA coexpression network. Diamond represents circRNA and circle represents miRNA. Up and downregulated circRNAs are shown in yellow and blue color, respectively. Larger size of diamond represents higher fold change of circRNAs. Solid lines represent positive relationship and dash lines represent negative relationship. circRNAs, circular RNAs; miRNAs, microRNAs

GO and KEGG analyses were performed to further annotate the biological functions of differentially expressed ncRNAs and their target genes. We noticed that a significant amount of GO and KEGG terms were related with endothelial or epithelial cell development which is closely involved in alveoli and pulmonary vessels development. This phenomenon is in accordance with the new BPD theory which shows that the core pathogenesis of BPD is simple alveolar structure and pulmonary microvascular abnormalities. Pulmonary angiogenesis and vascular development require the participation of various cytokines and signaling pathways, the most important of which include the VEGF/VEGFR pathway, Ang/Tie pathway, Ephrins/Eph pathway, and Notch/Jagged1 pathway.[36] These cytokines and signaling pathways play important roles in pulmonary vascular development. From our result (Figure 4), we also figured out that the Notch signaling pathway, VEGF signaling pathway, cytokines such as Interleukin-2 (IL-2) production were on the top 10 terms.

lncRNAs, with a transcript ranging from 200 nt to 100 kb, have drawn wide attention in the past decade.[37] A large number of lncRNAs have been identified to regulate oxidative stress, apoptosis, cell growth and viability, inflammation, and so on.[38-41] Instead of working alone, they coordinate with nearby (upstream or downstream) mRNAs.[37,42] So we performed a coexpression network of lncRNAs and mRNAs.

From the lncRNA-mRNA coexpression network (Figure 5), we found that lncRNA XLOC-067599 interacted with six mRNAs, including epidermal growth factor-like 6 (EGFL6), IL2, IL20rb, IL22ra2, IL24, and vascular endothelial growth factor C (VEGFC). Among them, VEGFC participates in the pathogenesis of BPD[43] through changing alveolar development. Abnormal expression of VEGFC

10974644, 2019, 6, Downloaded from https://onlinelibrary.wiley.com/doi/10.1002/jcb.28212 by Edinburgh University Library, Wiley Online Library on [05/08/2024]. See the Terms and Conditions (https://onlinelibrary.wiley.com/terms-and-conditions) on Wiley Online Library for rules of use; OA articles are governed by the applicable Creative Commons License

could be a risk factor for BPD and pulmonary hypertension (PH).[44] As to EGFL6, Noh et al reported that EGFL6 can stimulate tumor angiogenesis,[45] while angiogenesis is also a pathological process in BPD. Therefore, we speculated that lncRNA XLOC-067599 may regulate the expression of VEGFC and EGFL6 in BPD.

circRNAs, widely found in human and animal cells, play an essential role in the transcriptional and posttranscriptional processes of gene expression.[46] Bearing covalently closed loops without 3′-cap and 5′-end, circRNAs are stable during the enzymatic degradation and fluid absorption.[47] Possible functions of circRNAs have been reported as regulators of splicing and transcription, miRNA sponges, protein binding, and RNA transport.[17-20] So we constructed a coexpression network of circRNAs and miRNAs to define their function.

From the circRNA-miRNA coexpression network (Figure 6), we found that circRNAchr1:177096967|177109738 had a positive correlation with 21 miRNAs and negative correlation with 12 miRNAs. Among them, Xing et al found that miR-33-5P, miR-25-3P, miR-92a-3P, miR-181b-5P, miR-34a-5P, and miR-22-3P were significantly differentially expressed in the rat BPD model,[32] indicating their participation in the pathogenesis of BPD. We further clarified the target genes of these miRNAs. Finally, AKT3 was pinpointed as one target gene of miR-181b-5P. AKT3 also induced cell apoptosis,[48,49] which is consistent with the result of GO and KEGG analysis indicating that apoptosis may be involved in the pathogenesis of BPD. Therefore, we conclude that chr1:177096967|17710973 may regulate the expression of AKT3 by monitoring miR-181b-5P sponge.

Unfortunately, this study did not carry out the validation of these newly predictable genes, it is necessary as the next step research. Homologous database analysis in human and mouse experiments will also be performed. We hope to develop therapeutic strategies for BPD at the level of genetics in the future.

ACKNOWLEDGMENTS

This study was supported by grants from the National Natural Science Foundation of China (No. 81741089); and the Nanjing Medical Science and Technique Development Foundation (No. 201605052). We thank Assistant Professor Yong-ke Cao at the School of Foreign Languages of Nanjing Medical University for kind advice in the manuscript preparation.

CONFLICTS OF INTEREST

Authors declare that there are no conflicts of interest.

ORCID

Juan Wang http://orcid.org/0000-0001-9103-3315
Xingyun Wang http://orcid.org/0000-0002-8707-172X
Bin Zhuang http://orcid.org/0000-0001-6232-6856

REFERENCES

1. Horbar JD, et al. Mortality and neonatal morbidity among infants 501 to 1500 grams from 2000 to 2009. *Pediatrics*. 2012;129(6):1019-1026.
2. Hilgendorff A, O'Reilly MA. Bronchopulmonary dysplasia early changes leading to long-term consequences. *Front Med (Lausanne)*. 2015;2:2.
3. Baraldi E, Filippone M. Chronic lung disease after premature birth. *N Engl J Med*. 2007;357(19):1946-1955.
4. Jobe AH. The new bronchopulmonary dysplasia. *Curr Opin Pediatr*. 2011;23(2):167-172.
5. Hadchouel A, Delacourt C. Bronchopulmonary dysplasia and genetics. *Med Sci (Paris)*. 2013;29(10):821-823.
6. Silva DMG, Nardiello C, Pozarska A, Morty RE. Recent advances in the mechanisms of lung alveolarization and the pathogenesis of bronchopulmonary dysplasia. *Am J Physiol Lung Cell Mol Physiol*. 2015;309(11):L1239-L1272.
7. Yang Y, Qiu J, Kan Q, Zhou XG, Zhou XY. MicroRNA expression profiling studies on bronchopulmonary dysplasia: a systematic review and meta-analysis. *Genet Mol Res*. 2013;12(4):5195-5206.
8. Bao TP, Wu R, Cheng HP, Cui XW, Tian ZF. Differential expression of long non-coding RNAs in hyperoxia-induced bronchopulmonary dysplasia. *Cell Biochem Funct*. 2016;34(5):299-309.
9. Dang RY, Liu FL, Li Y. Circular RNA hsa_circ_0010729 regulates vascular endothelial cell proliferation and apoptosis by targeting the miR-186/HIF-1alpha axis. *Biochem Biophys Res Commun*. 2017;490(2):104-110.
10. Tang L, Chen HY, Hao NB, et al. microRNA inhibitors: Natural and artificial sequestration of microRNA. *Cancer Lett*. 2017;407:139-147.
11. Salmena L, Poliseno L, Tay Y, Kats L, Pandolfi PP. A ceRNA hypothesis: the Rosetta Stone of a hidden RNA language? *Cell*. 2011;146(3):353-358.
12. Trapnell C, Roberts A, Goff L, et al. Differential gene and transcript expression analysis of RNA-seq experiments with TopHat and Cufflinks. *Nat Protoc*. 2012;7(3):562-578.
13. Gao Y, Wang J, Zhao F. CIRI: an efficient and unbiased algorithm for de novo circular RNA identification. *Genome Biol*. 2015;16:4.
14. Szabo L, Morey R, Palpant NJ, et al. Statistically based splicing detection reveals neural enrichment and tissue-specific induction of circular RNA during human fetal development. *Genome Biol*. 2015;16:126.
15. Prieto C, Risueño A, Fontanillo C, De Las Rivas J. Human gene coexpression landscape: confident network derived from tissue transcriptomic profiles. *PLoS One*. 2008;3(12):e3911.
16. Liu Z, Li X, Sun N, et al. Microarray profiling and co-expression network analysis of circulating lncRNAs and mRNAs associated with major depressive disorder. *PLoS One*. 2014;9(3):e93388.
17. Memczak S, Jens M, Elefsinioti A, et al. Circular RNAs are a large class of animal RNAs with regulatory potency. *Nature*. 2013;495(7441):333-338.

10974644, 2019, 6, Downloaded from https://onlinelibrary.wiley.com/doi/10.1002/jcb.28212 by Edinburgh University Library, Wiley Online Library on [05/08/2024]. See the Terms and Conditions (https://onlinelibrary.wiley.com/terms-and-conditions) on Wiley Online Library for rules of use; OA articles are governed by the applicable Creative Commons License

18. Burd CE, Jeck WR, Liu Y, Sanoff HK, Wang Z, Sharpless NE. Expression of linear and novel circular forms of an INK4/ARF-associated non-coding RNA correlates with atherosclerosis risk. *PLoS Genet*. 2010;6(12):e1001233.
19. Jeck WR, Sorrentino JA, Wang K, et al. Circular RNAs are abundant, conserved, and associated with ALU repeats. *RNA*. 2013;19(2):141-157.
20. Qu S, Yang X, Li X, et al. Circular RNA: a new star of noncoding RNAs. *Cancer Lett*. 2015;365(2):141-148.
21. Bhandari V, Gruen JR. The genetics of bronchopulmonary dysplasia. *Semin Perinatol*. 2006;30(4):185-191.
22. Shaw GM, O'Brodovich HM. Progress in understanding the genetics of bronchopulmonary dysplasia. *Semin Perinatol*. 2013; 37(2):85-93.
23. Wang C, Gong B, Bushel PR, et al. The concordance between RNA-seq and microarray data depends on chemical treatment and transcript abundance. *Nat Biotechnol*. 2014;32(9):926-932.
24. Natarajan V, Ha AW, Dong Y, et al. Expression profiling of genes regulated by sphingosine kinase1 signaling in a murine model of hyperoxia induced neonatal bronchopulmonary dysplasia. *BMC Genomics*. 2017;18(1):664.
25. Peng R, Sridhar S, Tyagi G, et al. Bleomycin induces molecular changes directly relevant to idiopathic pulmonary fibrosis: a model for "active" disease. *PLoS One*. 2013;8(4):e59348.
26. Ratner V, Sosunov SA, Niatsetskaya ZV, Utkina-Sosunova IV, Ten VS. Mechanical ventilation causes pulmonary mitochondrial dysfunction and delayed alveolarization in neonatal mice. *Am J Respir Cell Mol Biol*. 2013;49(6):943-950.
27. Gauldie J, Galt T, Bonniaud P, Robbins C, Kelly M, Warburton D. Transfer of the active form of transforming growth factor-beta 1 gene to newborn rat lung induces changes consistent with bronchopulmonary dysplasia. *Am J Pathol*. 2003;163(6):2575-2584.
28. Capoluongo E, Ameglio F, Zuppi C. Insulin-like growth factor-I and complications of prematurity: a focus on bronchopulmonary dysplasia. *Clin Chem Lab Med*. 2008; 46(8):1061-1066.
29. Asikainen TM, Waleh NS, Schneider BK, Clyman RI, White CW. Enhancement of angiogenic effectors through hypoxia-inducible factor in preterm primate lung in vivo. *Am J Physiol Lung Cell Mol Physiol*. 2006;291(4):L588-L595.
30. Costa FF. Non-coding RNAs: meet thy masters. *BioEssays*. 2010;32(7):599-608.
31. Knowling S, Morris KV. Non-coding RNA and antisense RNA. Nature's trash or treasure? *Biochimie*. 2011;93(11):1922-1927.
32. Xing Y, FU J, YANG H, et al. MicroRNA expression profiles and target prediction in neonatal Wistar rat lungs during the development of bronchopulmonary dysplasia. *Int J Mol Med*. 2015;36(5):1253-1263.
33. Zhu X, Wang X, Wei S, et al. hsa_circ_0013958: a circular RNA and potential novel biomarker for lung adenocarcinoma. *FEBS J*. 2017;284(14):2170-2182.
34. Miao R, et al. Microarray expression profile of circular RNAs in chronic thromboembolic pulmonary hypertension. *Medicine*. 2017;96(27):e7354.
35. Bachmayr-Heyda A, Reiner AT, Auer K, et al. Correlation of circular RNA abundance with proliferation--exemplified with colorectal and ovarian cancer, idiopathic lung fibrosis, and normal human tissues. *Sci Rep*. 2015;5:8057.
36. Ma XN, Li QP, Feng ZC. Research progress in cytokines and signaling pathways for promoting pulmonary angiogenesis and vascular development. *Zhongguo Dang Dai Er Ke Za Zhi*. 2013;15(9):800-805.
37. Ponting CP, Oliver PL, Reik W. Evolution and functions of long noncoding RNAs. *Cell*. 2009;136(4):629-641.
38. Zeng Q, Wang Q, Chen X, et al. Analysis of lncRNAs expression in UVB-induced stress responses of melanocytes. *J Dermatol Sci*. 2016;81(1):53-60.
39. Huang S, Lu W, Ge D, et al. A new microRNA signal pathway regulated by long noncoding RNA TGFB2-OT1 in autophagy and inflammation of vascular endothelial cells. *Autophagy*. 2015;11(12):2172-2183.
40. Lu W, Huang SY, Su L, Zhao BX, Miao JY. Long Noncoding RNA LOC100129973 suppresses apoptosis by targeting miR-4707-5p and miR-4767 in vascular endothelial cells. *Sci Rep*. 2016;6:21620.
41. Yang Q, Xu E, Dai J, et al. A novel long noncoding RNA AK001796 acts as an oncogene and is involved in cell growth inhibition by resveratrol in lung cancer. *Toxicol Appl Pharmacol*. 2015;285(2):79-88.
42. Mattick JS, Gagen MJ. The evolution of controlled multitasked gene networks: the role of introns and other noncoding RNAs in the development of complex organisms. *Mol Biol Evol*. 2001;18(9):1611-1630.
43. Bhandari A, Bhandari V. Biomarkers in bronchopulmonary dysplasia. *Paediatr Respir Rev*. 2013;14(3):173-179.
44. Rivera L, Siddaiah R, Oji-Mmuo C, Silveyra GR, Silveyra P. Biomarkers for bronchopulmonary dysplasia in the preterm infant. *Front Pediatr*. 2016;4:33.
45. Noh K, Mangala LS, Han HD, et al. Differential effects of EGFL6 on tumor versus wound angiogenesis. *Cell Rep*. 2017;21(10):2785-2795.
46. Hou LD, Zhang J. Circular RNAs: an emerging type of RNA in cancer. *Int J Immunopathol Pharmacol*. 2017;30(1):1-6.
47. Fischer JW, Leung AKL. CircRNAs: a regulator of cellular stress. *Crit Rev Biochem Mol Biol*. 2017;52(2):220-233.
48. Sui J, Yang RS, Xu SY, et al. Comprehensive analysis of aberrantly expressed microRNA profiles reveals potential biomarkers of human lung adenocarcinoma progression. *Oncol Rep*. 2017;38(4):2453-2463.
49. Shin K, et al. Expression of interactive genes associated with apoptosis and their prognostic value for ovarian serous adenocarcinoma. *Adv Clin Exp Med*. 2016;25(3):513-521.

How to cite this article: Wang J, Yin J, Wang X, et al. Changing expression profiles of mRNA, lncRNA, circRNA, and miRNA in lung tissue reveal the pathophysiological of bronchopulmonary dysplasia (BPD) in mouse model. *J Cell Biochem*. 2019;120:9369-9380. https://doi.org/10.1002/jcb.28212

10974644, 2019, 6, Downloaded from https://onlinelibrary.wiley.com/doi/10.1002/jcb.28212 by Edinburgh University Library, Wiley Online Library on [05/08/2024]. See the Terms and Conditions (https://onlinelibrary.wiley.com/terms-and-conditions) on Wiley Online Library for rules of use; OA articles are governed by the applicable Creative Commons License